38157

LIBRARY
RESEARCH LABORATORIES
GENERAL MOTORS CORPORATION
FILE COPY

83IL21 #2

RESEARCH REPORT

EV-211

ABSOLUTE RATE CONSTANTS FOR THE REACTION OF OH WITH AMMONIA FROM 297-364 K

Robert D. Stephens
Environmental Science Department

September 21, 1983
29 pages

GM
General Motors
Research Laboratories
Warren, Michigan 48090

GM RESTRICTED ..... SEE TITLE PAGE FOR DISTRIBUTION LIMITS

GMR 247C
Rev. 3-78

RESEARCH REPORT NO. ● EV-211

Title ● Absolute Rate Constants for the Reaction of OH with Ammonia from 297-364 K

Date ● September 21, 1983

Reported by ● Robert D. Stephens

Approved by ● J. M. Heuss, Asst. Head, Environmental Science

General Motors Research Laboratories
Warren, Michigan 48090

GM RESTRICTED:

Title ■ May □ May Not Be Announced Within GMR
Title ■ May □ May Not Be Announced Within GM

PURPOSE

The purpose of this research was to measure the rate constant for the reaction of hydroxyl radicals with ammonia as a function of temperature.

SUMMARY

The oxidation of ammonia could be a significant source or sink for tropospheric NO_x via reactions of the NH_2 radical. This radical is formed in the troposphere predominantly by the reaction:

$$NH_3 + OH \rightarrow NH_2 + H_2O$$

This abstraction reaction is the rate-limiting step in the gas-phase oxidation of ammonia in the atmosphere. Numerous studies of this reaction have been undertaken, employing a variety of techniques. In this study, the discharge flow technique with resonance fluorescence detection of OH was used for the measurement of the rate constant as a function of temperature. Special attention was given to the minimization of secondary chemistry which could interfere with the measurement. The rate constant was measured at five temperatures from 297-364 K yielding the Arrhenius expression $(4.55 \pm 1.0) \times 10^{-12} \exp[(-973 \pm 78)/T]$ cm^3 $molec^{-1}$ s^{-1} with one standard deviation quoted as the statistical uncertainty. A comparison of this result to other reported values shows good agreement in most cases. A computer model of the experimental data was used to estimate rate constants for the reactions

$$NH_2 + NO \rightarrow N_2 + H + OH$$

$$NH_2 + NO_2 \rightarrow N_2 + 2\ OH$$

A Stern-Volmer analysis of the steady state OH fluorescence intensity measurements made during the OH + NH_3 rate constant experiments was used to determine the rate constant for $OH(A^2\Sigma^+)$ quenching by ammonia of $(9.6 \pm 0.8) \times 10^{-10}$ cm^3 $molec^{-1}$ s^{-1} at 297 K.

INTRODUCTION

Ammonia is the third most abundant nitrogen species in the atmosphere. It is thought to play a significant role in both homogeneous and heterogeneous atmospheric acid neutralization reactions.[1,2] However, possibly as much as 50% of atmospheric ammonia is oxidized in the gas phase.[3,4] The primary reaction responsible for the initial step in ammonia oxidation is:[4]

$$NH_3 + OH \rightarrow NH_2 + H_2O \qquad (1)$$

Several measurements of the rate constant for this reaction have been reported in the literature ranging from 4.1×10^{-14} to 2.7×10^{-13} cm^3 $molec^{-1}$ s^{-1} at room temperature.[5-12]

The ultimate fate of the amidogen radical (NH_2) thus formed is unclear, however. It has been implicated as a potentially significant source for atmospheric NO_x via the reactions:[1,4,6]

$$NH_2 + O_2 \rightarrow \text{products} \qquad (2)$$

$$NH_2 + O_3 \rightarrow \text{products} \qquad (3)$$

Unambiguous rate constant measurements for reaction (2) do not exist, but upper limits have been reported in the range 8.3×10^{-15} to 2×10^{-18} cm^3 $molec^{-1}$ s^{-1} at room temperature and above.[11,13,14] Rate constants for reaction (3) have been reported in the range 6.3×10^{-14} to 1.2×10^{-13} cm^3 $molec^{-1}$ s^{-1} at room temperature.[15,16,17]

The amidogen radical could also be a significant sink for atmospheric NO_x[1,4,6] via the reactions:

$$NH_2 + NO \rightarrow \text{products} \qquad (4)$$

$$NH_2 + NO_2 \rightarrow \text{products} \qquad (5)$$

The rate constant for reaction (4) has been reported in the range of 1.2×10^{-11} to 2.7×10^{-11} cm^3 $molec^{-1}$ s^{-1} at room temperature,[18-22] whereas reaction (5) has a rate constant measured to be 1.2×10^{-11} to 2.3×10^{-11} cm^3 $molec^{-1}$ s^{-1}.[19,24] Several possible exothermic channels exist for reactions (2)-(5), but few product identifications have been made. It is likely that reactions (3) and (4) occur by more than one pathway. For example, OH has been detected at levels of a few percent of NH_2 in experiments performed on reaction (3),[16] and perhaps 20% of reaction (4) proceeds via an OH formation process.[18] The formation of OH as a product of reaction (5) is also thermodynamically possible. Clearly, further study is required to elucidate the rates and mechanisms of potential atmospheric reactions of NH_2.

Given the rate constant measurements for reactions (1)-(5) and the approximate atmospheric concentrations of OH, NH_3, and NO_x, it can be concluded that the rate limiting step in ammonia oxidation is reaction (1).[12] It is, therefore, important that the rate constant for this reaction be accurately established. The initial objective in studying NH_x chemistry was, therefore, to unambiguously ascertain the rate constant of this reaction as a function of temperature.

EXPERIMENTAL

The discharge flow apparatus used in this study is illustrated in Fig. 1. It consists of a resonance fluorescence detection cell and a removable 2.5-cm I.D. x 3.8-cm O.D. Teflon-coated aluminum tube. Eight fixed-position reactant inlet tubes (1/16" O.D.) were equally spaced from 10 to 45 cm from the detection zone and were positioned to open at or near the center of the axis of major gas flow. Other ports were used for pressure and temperature measurements as well as for a sidearm through which radicals were introduced. The flow tube and fluorescence cell were wrapped with an electrical heating element and insulation. A movable thermocouple probe (retracted during kinetics measurements) was used to verify that temperature control was maintained to within ±2 K throughout the reaction zone.

Hydroxyl radicals were produced 30 cm upstream of the first reactant inlet port by reacting atomic hydrogen (produced by microwave discharge through 92-ppm hydrogen in helium) with an excess of nitrogen dioxide. Concentrations of nitrogen dioxide were chosen such that hydroxyl radical formation was always complete (i.e., three H atom half-lives) within three milliseconds.

Hydroxyl radicals were detected downstream via resonance fluorescence induced by a resonance lamp consisting of a microwave discharge through approximately two torr of 1% H_2O in helium. Fluorescence signals were collected at right angles to the fluorescence excitation source through an interference filter and detected via a photomultiplier (EMI 9789QA) operated in the

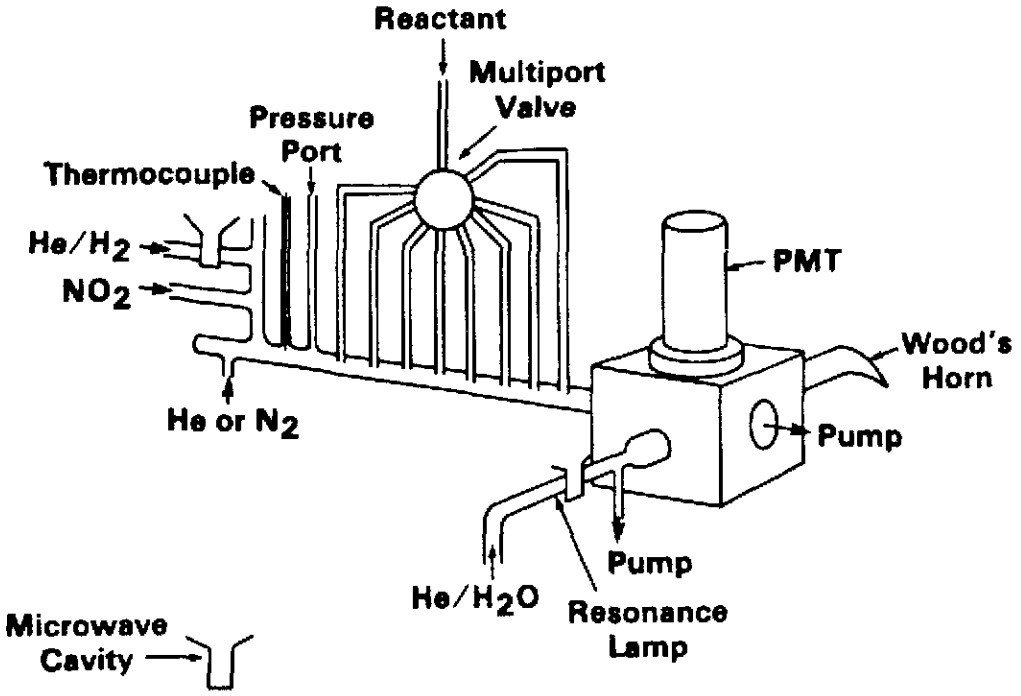

Fig. 1 Schematic diagram of discharge flow-resonance fluorescence system.

photon-counting mode. Apertures and focusing optics were utilized with both optical axes to maximize the ratio of signal to scattered light. Hydroxyl radical sensitivity was estimated at 3×10^9 molec cm^{-3} at a signal to noise ratio of one. Concentrations of hydroxyl radicals were measured daily by titration of H atoms with nitrogen dioxide, and never exceeded 6×10^{11} molecules cm^{-3}.

The clean Teflon-coated surface of the flow tube was found to have unacceptably high and irreproducible wall loss rates for hydroxyl radicals. Coating the flow tube and injectors with halocarbon wax (Halocarbon Products Corp. series 15-00) minimized this problem and was used for all experiments. Wall loss rates for hydroxyl were measured daily by varying the point of nitrogen dioxide injection and determining the slope of ln [OH fluorescence] vs. wall exposure time. Wall loss rates measured in this way never exceeded 6 s^{-1}. This technique assumes instantaneous hydroxyl formation, no H-atom wall loss, and no hydroxyl loss due to reaction with excess nitrogen dioxide. The first two assumptions lead to an underestimation of hydroxyl wall loss. This underestimate is partially offset by the reaction of hydroxyl with nitrogen dioxide which, under the conditions employed, occurs at approximately 1 s^{-1}. Hydroxyl wall loss rates were also determined from the intercepts of plots of pseudo-first-order decay rates of OH fluorescence vs. reactant concentration. Hydroxyl wall loss rates determined in this manner never exceeded 13 s^{-1}.

Gases used were helium (Matheson UHP 99.999%), hydrogen in helium (92-ppm Matheson certified standard), nitrogen dioxide in helium (274 ppm and 0.917% Matheson certified standard), and ammonia (Matheson anhydrous 99.99% minimum). The 0.917% nitrogen dioxide in helium was analyzed via long path Fourier

transform infrared spectroscopy and found to contain 550 ppm of nitric oxide as a contaminant. All gases were used directly without further purification.

Pressure in the flow system was measured at 50 cm from the detection zone by an MKS capacitance manometer. Temperature was measured with type-T thermocouples. All gas flow rates were controlled and measured with Tylan mass-flow controllers calibrated by measuring the pressure rise resulting from a timed flow into a known volume.

The kinetics experiments were performed under pseudo-first-order conditions by adding ammonia in large excess over hydroxyl, sequentially through each of the eight reactant inlet ports. Measurements of scattered light and OH fluorescence in the absence of ammonia, I_F°, were made both immediately before and after the kinetics experiments were conducted. Measurements of I_F° were used in the determination of the rate constant for quenching of OH ($A^2\Sigma^+$) by ammonia as discussed later.

Acquisition of fluorescence count rates, gas flow rates, pressure, and temperature was accomplished by a CAMAC standard Kinetic Systems 8010 microcomputer system. Statistical tests were applied to these measurements to verify that data collection occurred during stable experimental conditions. A series of eight measurements of each parameter was made at each reaction time and the data remeasured if the standard deviation in any measurement was greater than 3%. Remeasurement of data was typically not required under these conditions.

The measured pressure and calculated flow velocity were corrected for viscous pressure drop to derive the pressure and velocity at the point

representing the average of the midpoints between reactant injection and hydroxyl detection. These corrections were typically approximately 5%. The corrected flow velocity (typically 20 m s^{-1}) and pressure (~1 torr) were used to calculate the reaction time and species concentrations (based on the fraction of total flow measured for each gas).

RESULTS

$OH + NH_3$

Reaction (1) was studied at five temperatures from 297 to 364 K at 1 torr. With $[NH_3] > 1.4 \times 10^{14}$ molec $cm^{-3} \gg [OH] \leq 6 \times 10^{11}$ molec cm^{-3}, reaction (1) is pseudo-first-order in OH. Figure 2 shows typical plots of ln [OH fluorescence] vs. reaction time. Slopes of such plots yield a value for the observed pseudo-first-order rate of OH decay, K_{OBS}, where $K_{OBS} = k_1[NH_3] + k_w$ and k_w is a first-order term for removal of OH at the flow tube wall. Intercepts of such plots yield a value for the fluorescence intensity, I_F, in the presence of ammonia but in the absence of OH removal by reaction with ammonia. The values for I_F were employed in a Stern-Volmer analysis as discussed later. A plot of K_{OBS} vs. $[NH_3]$ is shown in Fig. 3. The value for k_1 at each temperature is derived from the slope of such plots as calculated by a weighted least-squares fit of the data. The value for k_1 at 297 K determined in this way is $1.73 \pm 0.11 \times 10^{-13}$ cm^3 $molec^{-1}$ s^{-1}. A summary of K_{OBS}, temperature, and ammonia concentration for each experiment, as well as the values of k_1 are listed in Table I.

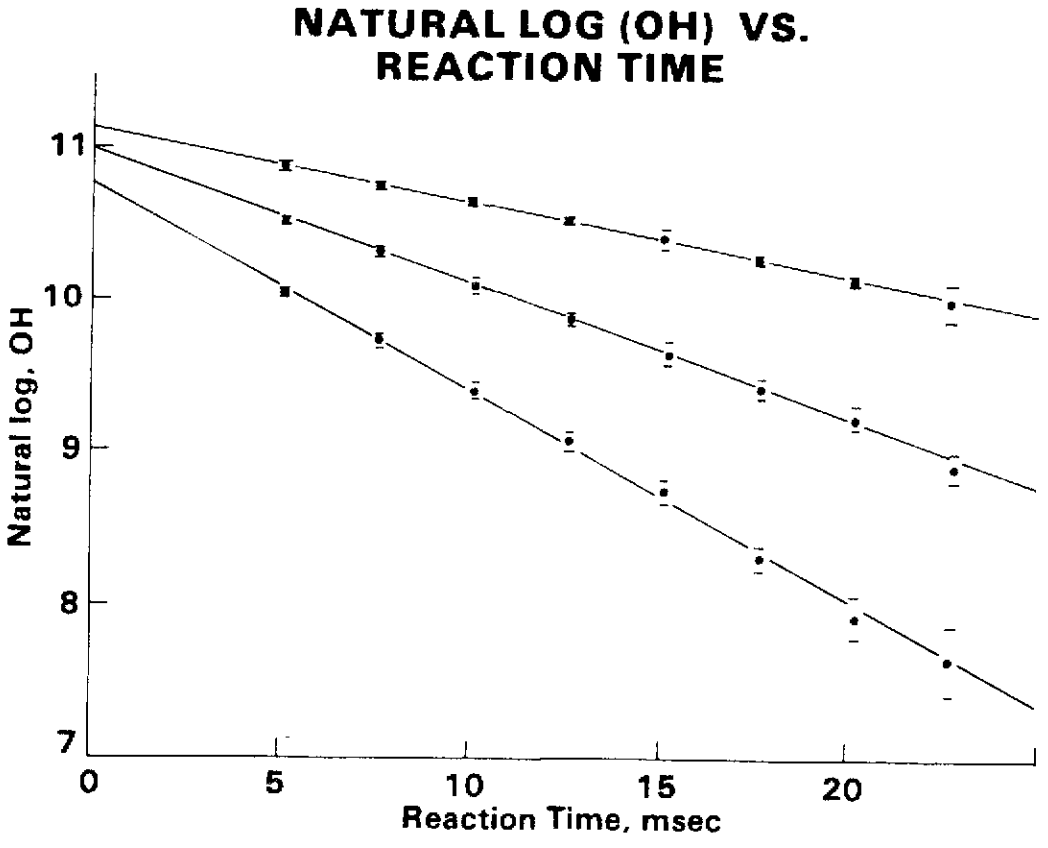

Fig. 2 Plots of the natural log of OH fluorescence signal vs. reaction time at 334 K. The curves shown correspond to 1.61×10^{14}, 3.01×10^{14} and 5.14×10^{14} molec cm^{-3} ammonia respectively from top to bottom. Error bars represent statistical uncertainties of 2σ. Intercepts of such plots represent the natural log of OH fluorescence intensity in the presence of ammonia but in the absence of OH removal by reaction with ammonia. This extrapolated value for fluorescence intensity, I_F, can be used in a Stern-Volmer analysis to yield the rate constant for quenching of $OH(A^2\Sigma^+)$ by ammonia as has been reported herein for 297 K data.

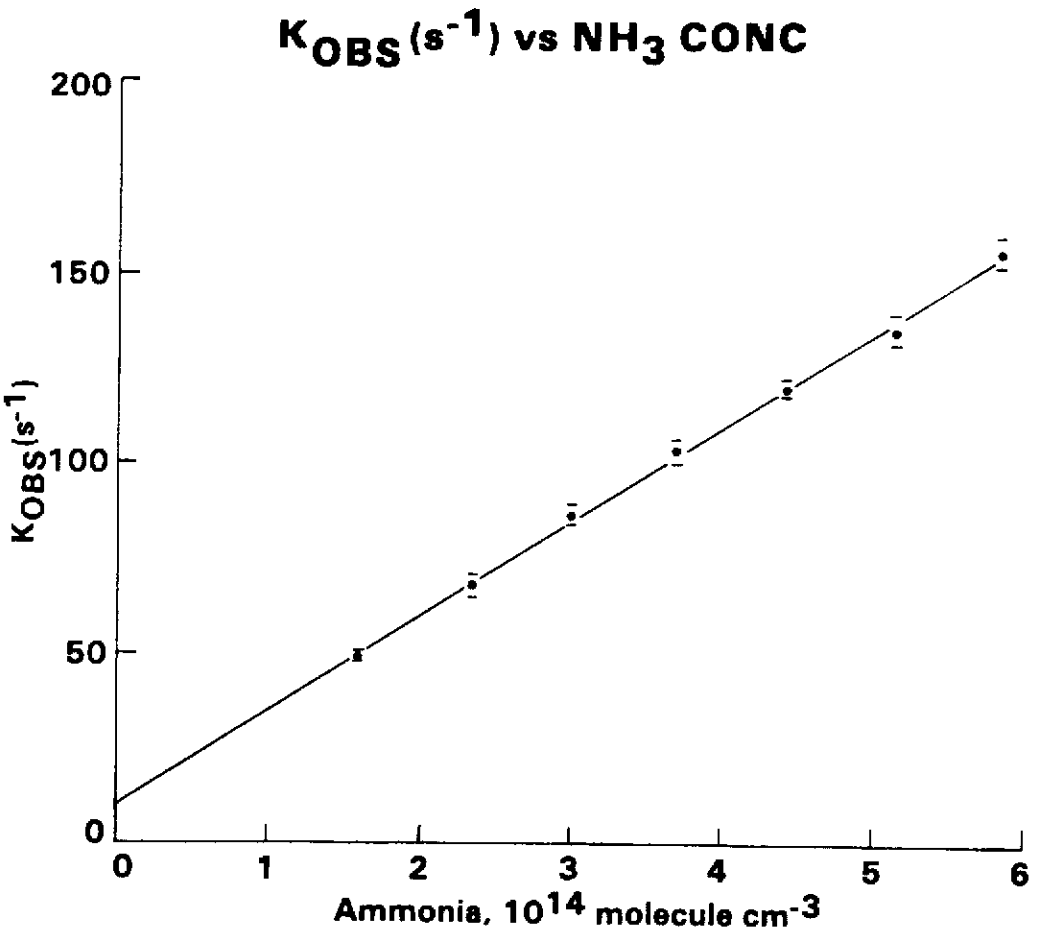

Fig. 3 Plot of pseudo-first-order rate constant for OH fluorescence decay vs. ammonia concentration. Data is for 334 K.

TABLE I

Compilation of Experimental Data from k_1 Determination

Temp. °K	$[NH_3]$ 10^{14} molec cm^{-3}	K_{OBS} s^{-1}	1 $\sigma_{K_{OBS}}$ s^{-1}	k_1 cm^3 $molec^{-1}$ s^{-1}
297	2.66	57.0	1	
297	4.33	88.5	2	
297	6.24	130	2	
297	7.91	148	2	
297	9.68	168	4	
297	11.4	195	4	
297				$(1.73 \pm 0.11) \times 10^{-13}$
320	2.11	56.8	1	
320	3.34	84.0	2	
320	4.18	105.0	2	
320	5.05	123	1	
320	5.92	140	2	
320	6.99	158	1	
320				$(2.12 \pm 0.06) \times 10^{-13}$
334	0.61	49.9	1	
334	2.30	68.2	2	
334	3.01	87.0	1	
334	3.71	104	2	
334	4.43	120	1	
334	5.14	136	2	
334	5.86	156	2	
334				$(2.48 \pm 0.03) \times 10^{-13}$
348	0.16	48.9	1	
348	2.14	64.3	1	
348	2.67	80.9	2	
347	3.21	101	2	
347	3.73	114	2	
347	4.24	119	1	
348				$(2.74 \pm 0.12) \times 10^{-13}$
363	1.47	32.2	1	
363	1.98	46.6	1	
363	2.50	59.6	1	
363	3.00	86.1	1	
363	3.54	98.4	1	
363	4.10	111	1	
363	4.59	125	1	
363				$(3.07 \pm 0.15) \times 10^{-13}$

The values for k_1 for the five temperatures were fit to an Arrhenius expression to yield a temperature-dependent rate constant of $(4.55 \pm 1.0) \times 10^{-12} \exp[(-973 \pm 78)/T]$ cm^3 $molec^{-1}$ s^{-1}. The stated errors in all cases represent one standard deviation. The Arrhenius plot is shown in Fig. 4.

OH ($A^2\Sigma^+$) Quenching

From Fig. 2 it can be noted that the OH fluorescence signal at zero reaction time varies as a function of ammonia concentration. Under ideal conditions resonance fluorescence would result from two processes:

$$h\nu + OH \rightarrow OH(A^2\Sigma^+) \qquad (a)$$

$$OH(A^2\Sigma^+) \xrightarrow{k_r} OH(X^2\Pi_i) + h\nu' \qquad (b)$$

where $h\nu'$ is the OH fluorescence to be detected and k_r is the rate constant for the radiative decay of $OH(A^2\Sigma^+)$. However, the nonradiative process of collisional quenching can also occur:

$$OH(A^2\Sigma^+) + M \xrightarrow{k_q^M} OH(X^2\Pi_i) + M \qquad (c)$$

where k_q^M is the rate constant for the quenching process via molecule M. Fluorescence intensity is, then, a function of quenching. Under the experimental conditions employed, M is predominantly helium, NO_2 and NH_3. The $OH(A^2\Sigma^+)$ fluorescence lifetime, τ_F°, in the absence of ammonia is

$$\tau_F^\circ = \left((k_r + k_q^{He}[He] + k_q^{NO_2}[NO_2]\right)^{-1}$$

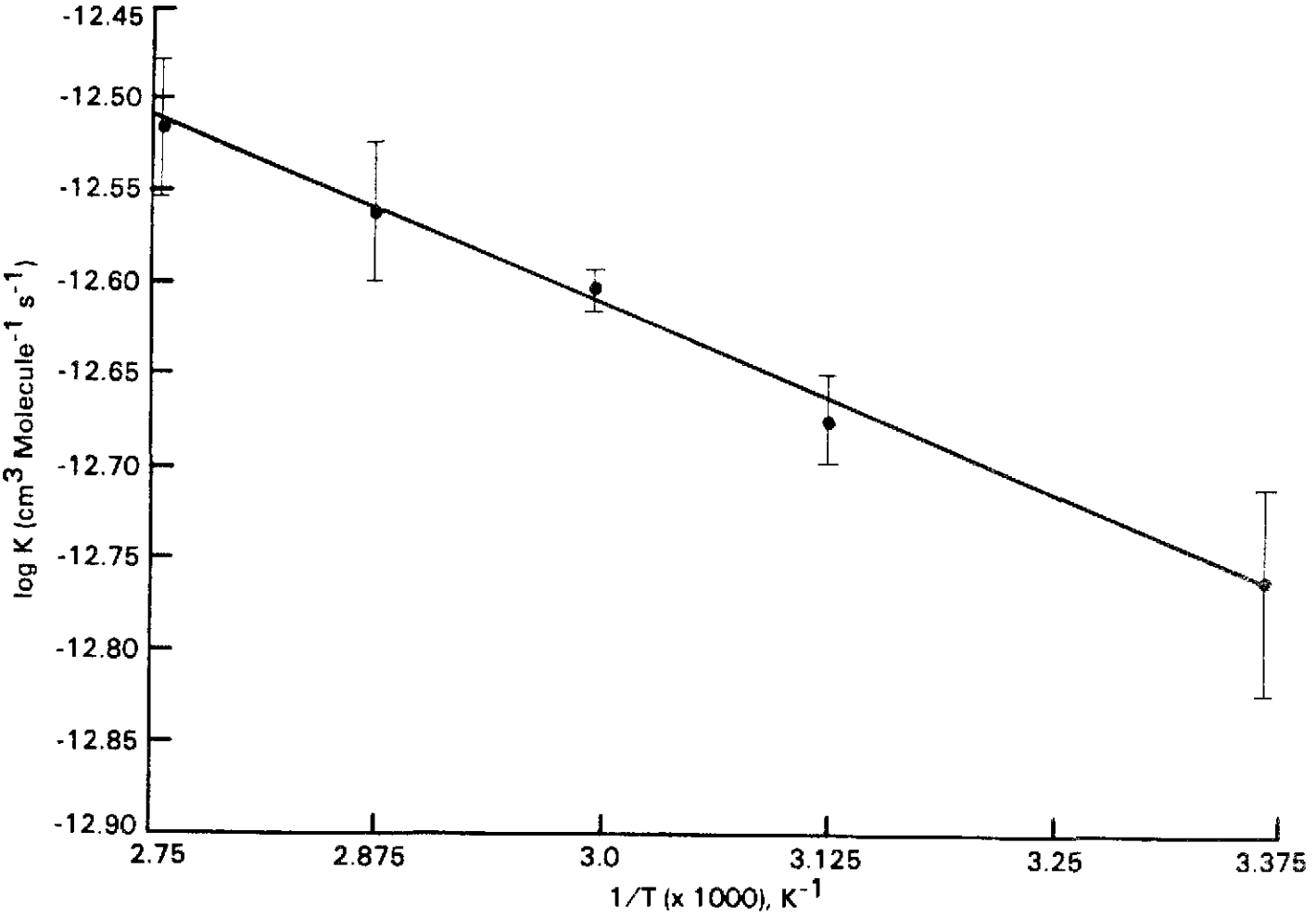

Fig. 4 Arrhenius plot for the temperature dependence of OH + NH_3 reaction rate constant. Error bars represent statistical uncertainties of 2 σ.

The $OH(A^2\Sigma^+)$ fluorescence lifetime in the presence of ammonia, τ_F, is:

$$\tau_F = \left(k_r + k_q^{He}[He] + k_q^{NO_2}[NO_2] + k_q^{NH_3}[NH_3]\right)^{-1}$$

At a given hydroxyl concentration, the ratio of OH fluorescence intensity in the absence of ammonia, I_F°, to the fluorescence intensity in the presence of ammonia, I_F, is:

$$I_F^\circ/I_F = \tau_F^\circ/\tau_F = 1 + \tau_F^\circ\, k_q^{NH_3}[NH_3]$$

This is the typical Stern-Volmer quenching expression which can be employed to derive a rate constant for the quenching of $OH(A^2\Sigma^+)$ by ammonia. The values of I_F used for these calculations were obtained in conjunction with the k_1 determination by extrapolating the ln(OH fluorescence) vs. reaction time data (Fig. 2) to zero reaction time. This provides a measure of OH fluorescence both in the presence of ammonia and in the absence of removal of OH by reaction with ammonia. The values for I_F° were the fluorescence signals measured in the absence of added ammonia. Ammonia flows used for the k_1 determination never exceeded 3% of total gas flow; hence, concentrations of other quenchers remained essentially constant between measurements of I_F° and experiments resulting in derivation of I_F.

Using the radiative lifetime of $OH(A^2\Sigma^+)$ and the rate constants for quenching of $OH(A^2\Sigma^+)$ summarized by Schofield,[23] the $OH(A^2\Sigma^+)$ fluorescence lifetime in the absence of ammonia (τ_F°) is essentially equal to the radiative lifetime of $OH(A^2\Sigma^+)$, i.e., $\sim 0.76 \times 10^{-6}$ s. Given the gas flow velocities employed in the experiments (~ 20 m s^{-1}) and the spatial resolution of fluorescence

detection (~0.5 cm), the time resolution of fluorescence detection is long relative to processes (a)-(c), hence these processes are in steady state.

A least-squares analysis of the data (Fig. 5) yields a value for $\tau_F^\circ k_q^{NH_3}$ of $(7.3 \pm 0.6) \times 10^{-16}$ cm^3 molec^{-1}. Hence the 297 K rate constant for $OH(A^2\Sigma^+)$ quenching, as measured relative to the radiative lifetime, is $(9.6 \pm 0.8) \times 10^{-10}$ cm^3 molec^{-1} s^{-1}. Although possible, there is no evidence that quenching involves chemical reactions. This possiblity was not investigated in these experiments. It should also be noted that the measurement of k_1 and k_q, although subject to the same uncertainties, are each independent of the other.

DISCUSSION

Data from experiments performed at room temperature and high ammonia concentrations displayed a slight nonlinearity in plots of ln (OH fluorescence) vs. reaction time as shown in Fig. 6. Although the data are linear within the statistical uncertainties, the slight nonlinearities are suggestive of an effect of secondary chemistry. The potential fate of NH_2 formed via reaction (1) was therefore investigated.

Recent studies have revealed two possible branches for reaction (4):

$$NH_2 + NO \rightarrow N_2 + H_2O \qquad (4a)$$

$$NH_2 + NO \rightarrow N_2 + H + OH \qquad (4b)$$

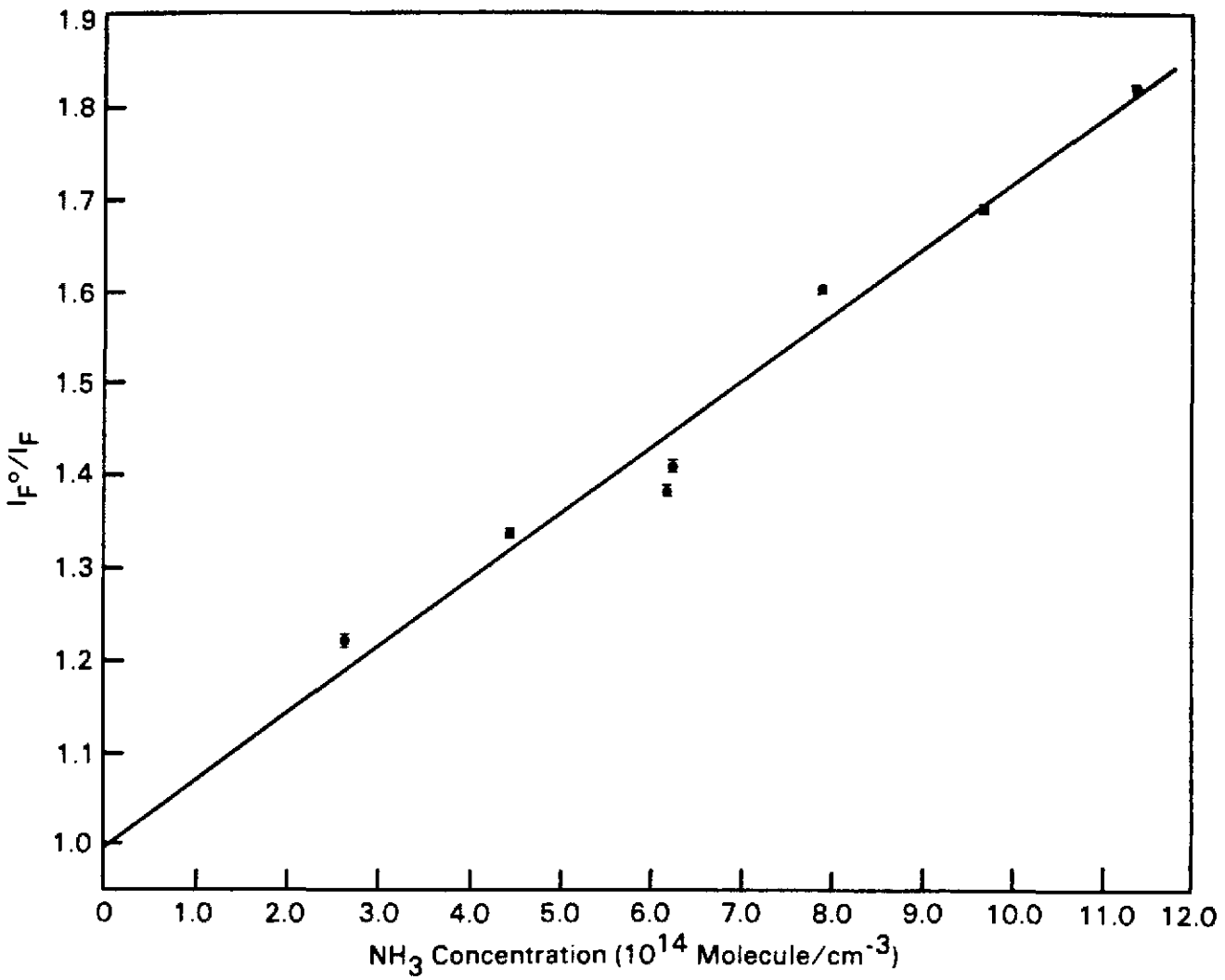

Fig. 5 Stern-Volmer plot of 297 K data showing $I_F°/I_F$ vs. ammonia concentration. Error bars represent statistical uncertainties of 2 σ.

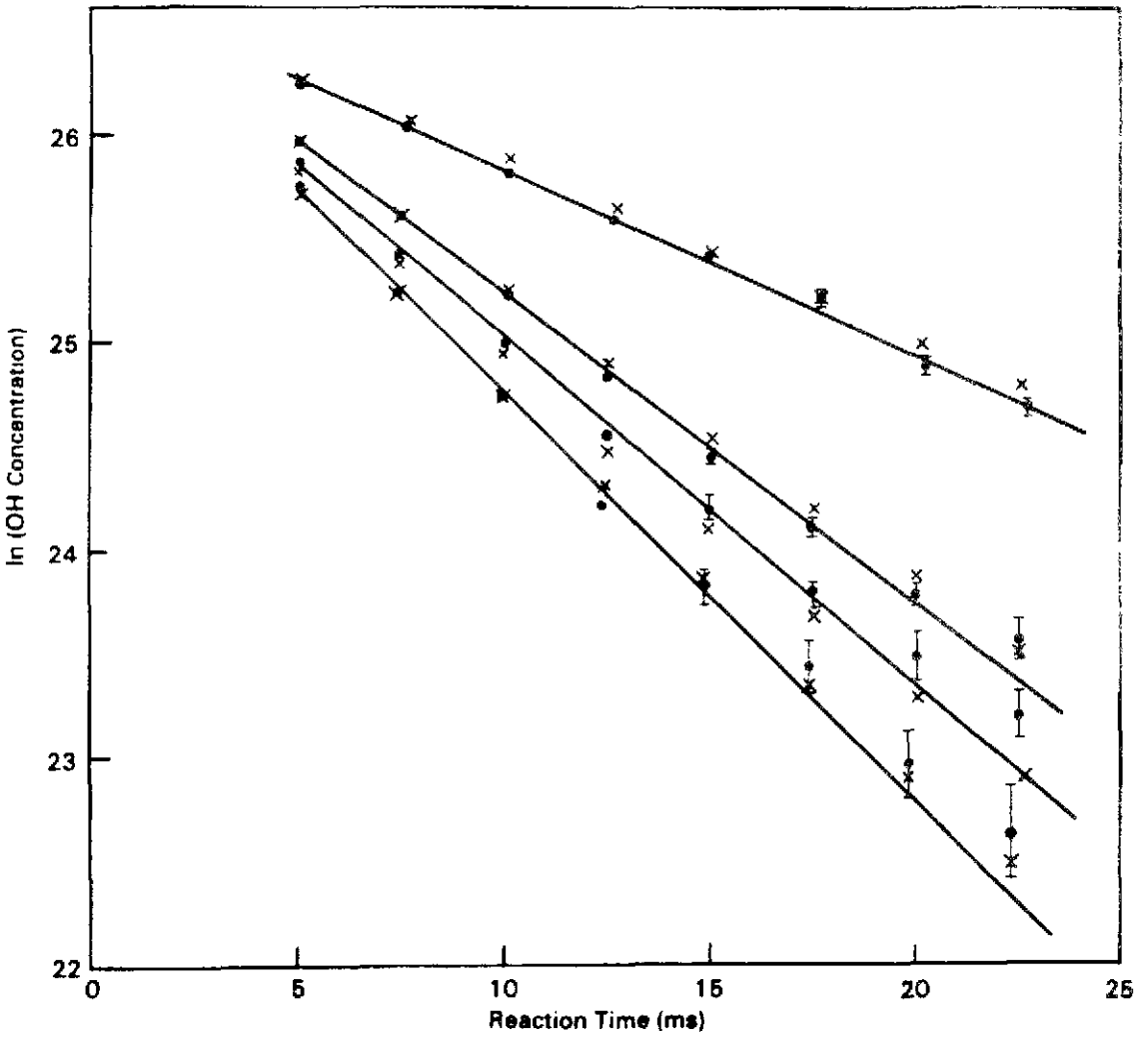

Fig. 6 Comparison of experimental data (normalized to measured OH concentration) and the computer model predictions of OH concentration. Solid lines represent the weighted least squares fit of experimental data (•). The computer model predictions of OH concentration (x) were obtained using $k_{4b} = 5 \times 10^{-12}$ cm^3 molec^{-1} s^{-1} and $k_{5b} = 0$ cm^3 molec^{-1} s^{-1}. Similar model predictions result with $k_{5b} = 5 \times 50^{-13}$ cm^3 molec^{-1} s^{-1} and $k_{4b} = 0$ cm^3 molec^{-1} s^{-1}. The curves represent ammonia concentrations (from top to bottom) of 4.33×10^{14}, 7.91×10^{14}, 9.68×10^{14}, and 1.14×10^{15} molec cm^{-3}. The increasing curvature with increasing ammonia concentration is possibly due to the faster rate of reaction (4b) and/or (5b) which results from increased NH_2 formation from reaction (1). The increased curvature of these plots relative to those of Fig. 2 suggests that the OH formation channels of reactions (4) and (5) have negative temperature dependences as has been previously observed for the overall reactions.

At room temperature, possibly 20% of reaction (4) occurs via (4b).[18] In these experiments, reaction (4b) would result in the production of two OH for each NH_2 reacted, since OH would also be formed via the fast reaction of H with the nitrogen dioxide in the system.

There is evidence that reaction (5) occurs predominantly but not exclusively via:[19]

$$NH_2 + NO_2 \rightarrow N_2O + H_2O \qquad (5a)$$

However, there is an exothermic channel for this reaction which could also result in OH formation:

$$NH_2 + NO_2 \rightarrow N_2 + 2\ OH \qquad (5b)$$

The potential impact of reactions (4b) and (5b) on measured OH decays in this study would therefore be nearly identical, i.e., two OH formed for each NH_2 reacted.

Reactions (4) and (5) have both been measured to have negative temperature dependences which would be consistent with the observation of nonlinearity of experimental data at low temperature only. Furthermore, this nonlinearity would be expected to be most prominent under conditions of high NH_2 concentration, which is consistent with its occurrence only in experiments performed using high ammonia concentrations.

To determine the possible influence of reactions (4b) and (5b) on the measurements reported herein, a computer model of the dominant chemistry present in the experiments was used to simulate the results at 297 K. The chemical reactions and rate constants used in the simulation are shown in Table II. The simulations were performed using a program written by M. R. Whitbeck[26] that uses the technique described by Gear.[25] Simulations were based on experiments at room temperature and utilized the measured [OH], k_w, [NO_2] and pressure. To determine the potential influence of reaction (5b) on the measurements reported herein, the rate constants for (5a) and (5b) were varied while maintaining the overall rate constant at $k_5 = 2.2 \times 10^{-11}$ cm^3 $molec^{-1}$ s^{-1} and assuming $k_{4b} = 0$. The model predicted the experimental K_{OBS} for hydroxyl when $k_{5b} = 5 \times 10^{-13}$ cm^3 $molec^{-1}$ s^{-1}. The model predicted OH concentrations outside the 2σ statistical uncertainties of the OH fluorescence measurements when $k_{5b} = 1 \times 10^{-12}$ cm^3 $molec^{-1}$ s^{-1}. To determine the potential impact of reaction (4b) on the measurement of k_1 the rate constants for (4a) and (4b) in the simulations were also varied while maintaining the overall rate constant at $k_4 = 2.2 \times 10^{-11}$ cm^3 $molec^{-1}$ s^{-1} and assuming $k_{5b} = 0$. The simulations indicate that the experimental results were relatively insensitive to the branching ratio of reaction (4) since the dominant loss of NH_2 was via reaction (5). However, the best match between the experimentally obtained K_{OBS} and K_{OBS} obtained from the simulation occurred when reaction (4b) was predicted to proceed at approximately 5×10^{-12} cm^3 $molec^{-1}$ s^{-1}. The simulation results are shown with experimental data in Fig. 6. The rate of OH formation predicted by the model from either reaction (4b) or (5b), is less than 10% of the rate of OH loss due to reaction (1) throughout the range of ammonia concentrations utilized in the experiments. Furthermore, the model predicts OH concentrations within the 2σ limits of statistical uncertainty of the experimental data when k_{4b} and k_{5b} are

TABLE II

Chemical model used to examine the perturbation on measured [OH] resulting from reaction (4b) or (5b). Initial concentrations:

$[NO] = 1 \times 10^{12}$ molec cm^{-3}*
$[NO_2] = 1 \times 10^{13}$ molec cm^{-3}
$[NH_3] = 4.33 \times 10^{14} - 1.14 \times 10^{15}$ molec cm^{-3}
$[M] = 3.2 \times 10^{16}$ molec cm^{-3}
$[OH] = 4 \times 10^{11}$ molec cm^{-3}

	Reaction	Rate Constant	References
	$H + NO_2 \rightarrow OH + NO$	1.23×10^{-10} cm^3 $molec^{-1}$ s^{-1}	28
	$OH + NH_3 \rightarrow NH_2 + H_2O$	1.7×10^{-13} cm^3 $molec^{-1}$ s^{-1}	This work
(4a)	$NH_2 + NO \rightarrow N_2 + H_2O$	$0\text{-}2.2 \times 10^{-11}$ cm^3 $molec^{-1}$ s^{-1}	Sum of 4a and 4b set at average of references 20, 21 and 22
(4b)	$NH_2 + NO \rightarrow N_2 + H + OH$	$2.2 \times 10^{-11} - 0$ cm^3 $molec^{-1}$ s^{-1}	
(5a)	$NH_2 + NO_2 \rightarrow N_2O + H_2O$	$2.2 \times 10^{-11} - 0$ cm^3 $molec^{-1}$ s^{-}	Sum of 5a and 5b set at average of references 19 and 24
(5b)	$NH_2 + NO_2 \rightarrow N_2 + 2\ OH$	$0\text{-}2.2 \times 10^{-11}$ cm^3 $molec^{-1}$ s^{-1}	
	$NH_2 + H + M \rightarrow NH_3 + M$	2.9×10^{-30} cm^6 $molec^{-2}$ s^{-1}	29
	$NH_2 + NH_2 + M \rightarrow N_2H_4 + M$	6.9×10^{-30} cm^6 $molec^{-2}$ s^{-1}	29
	$NH_2 + OH \rightarrow NH_2OH$	5.0×10^{-11} cm^3 $molec^{-1}$ s^{-1}	14
	$OH + NO_2 + M \rightarrow HNO_3 + M$	2.6×10^{-30} cm^6 $molec^{-2}$ s^{-1}	28
	$OH + NO + M \rightarrow HONO + M$	6.7×10^{-31} cm^6 $molec^{-2}$ s^{-1}	27
	$OH + OH \rightarrow H_2O + O$	1.8×10^{-12} cm^3 $molec^{-1}$ s^{-1}	28
	$OH \rightarrow WALL$	12.6 s^{-1}	This work
	$NH_2 \rightarrow WALL$	12.6 s^{-1}	Assumed equal to k_w for OH as measured in this work

* Based on the measured NO contamination of the NO_2 used, plus the NO resulting from the OH formation reaction.

both zero. The modelling of these experiments therefore suggests that OH formation from NH_2 reactions is possible if not probable.* However, the data demonstrate that k_1 is not significantly perturbed by this secondary chemistry.

Of seven studies of k_1 previously reported (summarized in Table III), four are in reasonable agreement and yield the preferred value for k_1 of 1.6×10^{-13} cm^3 $molec^{-1}$ s^{-1} at room temperature.[30] Three of four flash photolysis studies[5-7] and one of two discharge flow studies[9] support this result.

A potential for secondary chemistry in the flash photolysis studies exists due to the potential for ammonia photolysis with subsequent reaction of the NH_2 photofragment via:

$$NH_2 + OH \rightarrow \text{products} \qquad (6)$$

The rate constant for reaction (6) has been estimated at 5×10^{-11} cm^3 $molec^{-1}$ s^{-1}.[14] Since the absorption cross section for ammonia, across much of the ultraviolet spectrum,[27] is equal to or greater than that for water (the OH source in most flash photolysis studies), the concentration of NH_2 produced by both photolysis and reaction (1) could be expected to exceed the concentration of OH. Hence the rate of OH decay in the flash photolysis studies might be expected to increase beyond that resulting from reaction (1). However, Smith and Zellner[5] carefully checked for and eliminated this possible complication in

---

* In fact, preliminary experiments performed in this laboratory have confirmed the formation of OH (as detected via resonance fluorescence) from either reaction (4b) or (5b). Subsequent detection of nitric oxide contamination of the nitrogen dioxide used in these experiments precludes the confirmation of reaction (5b) as the sole source of this OH, however. Further investigations of these reactions are currently in progress.

TABLE III

A Comparison of Results of This Study to Previously Reported Values of k_1

Room Temperature Rate Constant (cm^3 $molecule^{-1}$ s^{-1})	A (cm^3 $molecule^{-1}$ s^{-1})	E (cal $mole^{-1}$)	Temperature Range (K)	Method	Ref.
1.57×10^{-13}	2.3×10^{-12}	1600	228 - 472	Flash photolysis resonance absorption	5
$1.5 (\pm 0.4) \times 10^{-13}$			298	Flash photolysis resonance fluorescence	6
$1.64 (\pm 0.16) \times 10^{-13}$	2.93×10^{-12}	1710 ± 300	297 - 427	Flash photolysis resonance fluorescence	7
$1.44 (\pm 0.29) \times 10^{-13}$	$(5.41 \pm 0.86) \times 10^{-12}$	2120 ± 143	294 - 1075	Discharge flow resonance fluorescence	9
2.42×10^{-13}	$(5.3 \pm 0.8) \times 10^{-12}$	1830	298 - 669	Discharge flow electron spin resonance	10
$(2.7 \pm 0.3) \times 10^{-13}$	1.1×10^{-12}	870 ± 80	298 - 365	Pulsed radiolysis kinetic spectroscopy	11
$(4.1 \pm 0.6) \times 10^{-14}$			298	Flash photolysis resonance fluorescence	12
$(1.73 \pm 0.11) \times 10^{-13}$	$(4.55 \pm 1.1) \times 10^{-12}$	1933 ± 155	297 - 364	Discharge flow resonance fluorescence	This work

their study. The agreement obtained in two of three other flash photolysis studies which did not investigate this possibility suggests that the rate constant for reaction (6) has been overestimated.

The possible complicating secondary chemistry in the discharge flow studies results from the potential for OH regeneration via reactions (4b) and (5b) as discussed previously. This would result in a decreased rate of OH decay from that expected due to reaction (1). Of the two discharge flow studies, only Hack et al.,[10] considered secondary chemistry. Their result, however, does not agree with the flash photolysis studies. The discharge flow study of Silver and Kolb[9] did not investigate secondary chemistry. Furthermore, the temperature range of their study is not comparable with the flash photolysis studies, except at room temperature where their result is in agreement.

This study, then, offers an alternative to the flash photolysis technique while also carefully considering potential secondary chemistry. The good agreement obtained between this study and most flash photolysis studies (despite the potential for secondary chemistry which could effect the results in opposite directions) offers strong confirmation for the preferred value of k_1.

As reaction (1) is the rate-limiting step in the atmospheric gas-phase oxidation of ammonia, it controls the extent to which the tropospheric NO_x budget can be influenced by reactions (2)-(5). The extent of this influence could far exceed NO_x sources due to combustion.[6] An understanding of this influence awaits knowledge concerning the relative importance of reactions (4) and (5) (NO_x sink) as opposed to reactions (2) and (3) (NO_x source), as well as the relative importance of reaction (1) to heterogeneous or other ammonia loss

processes. Further investigations of the rates and mechanisms of reactions (2)-(5) are, therefore, still required.

The technique employed to concurrently obtain the rate constant for $OH(A^2\Sigma^+)$ quenching and $OH(X^2\Pi_i)$ reaction kinetics has not, to the author's knowledge, been previously employed. A more cumbersome technique to accomplish this has been reported by Clyne and Holt.[31] However, it is worthwhile to note that the technique reported herein can be easily applied to much of the extensive data in existence for ground state radical reaction kinetics, with no further measurements required. Furthermore, this technique is equally valid for flash photolysis experiments. Care must be taken, however, to insure stable intensities in the fluorescence excitation and the photolysis source so as to maintain constant concentration and excitation of $OH(X^2\Pi_i)$ between measurements of I_F and I_F°. This means that the reactant must not significantly absorb either wavelength employed.

ACKNOWLEDGMENT

The author wishes to express his gratitude to Dr. Larry G. Anderson for his preparation of software used for data acquisition and analysis as well as for many helpful discussions, to Dr. David Dolson for his helpful review of this manuscript, and to Dr. Jerry D. Rogers for the gas analysis.

REFERENCES

1. S. C. Wofsy and M. B. McElroy, Can. J. Chem., 52, 1582 (1974).
2. T. E. Graedel, Chemical Compounds in the Atmosphere, Academic Press, New York, 1978.
3. "Report of the NASA Working Group on Tropospheric Program Planning," NASA Reference Publication 1062, 1980.
4. J. C. McConnell, J. Geophys. Res., 78, 7812 (1973).
5. I. W. M. Smith and R. Zellner, Int. J. Chem. Kinet. Symp., 1, 341 (1975).
6. F. Stuhl, J. Chem. Phys., 59, 635 (1973).
7. R. A. Perry, R. Atkinson, and J. N. Pitts, Jr., J. Chem. Phys., 64, 3237 (1976).
8. S. Gordon and W. A. Mulac, Int. J. Chem. Kinet. Symp., 1, 289 (1975).
9. J. A. Silver and C. E. Kolb, Chem. Phys. Letters, 75, 191 (1980).
10. V. W. Hack, K. Hoyermann and H. Gg. Wagner, Ber. Bunsenges Physik. Chem., 78, 386 (1974).
11. P. B. Pagsberg, J. Eriksen, and H. C. Christensen, J. Phys. Chem., 83, 582 (1979).
12. M. J. Kurylo, Chem. Phys. Letters, 23, 467 (1973).
13. R. Lesclaux and M. Demissy, Nouv. J. Chim., 1, 443 (1977).
14. S. G. Cheskis and O. M. Sarkisov, Chem. Phys. Letters, 62, 72 (1979).
15. H. Kurasawa and R. Lesclaux, Chem. Phys. Letters, 72, 437 (1980).
16. W. Hack, O. Horie and H. Gg. Wagner, Ber. Bunsenges Phys. Chem., 85, 72 (1981).
17. V. P. Bulatov, A. A. Buloyan, S. G. Cheskis, M. Z. Kozliner, O. M. Sarkisov and A. I. Trostin, Chem. Phys. Letters, 74, 288 (1980).

18. J. A. Silver, C. M. Gozewski, and C. E. Kolb, ARI-RR-216, Western States Section 1 Combustion Institute, October 20, 1980.

19. W. Hack, H. Schacke, M. Schröter, and H. Gg. Wagner, Seventeenth Symposium (International) on Combustion, The Combustion Institute, Pittsburgh, Pennsylvania, 1978, p. 505.

20. G. Hancock, W. Lange, M. Lenzi, and K. H. Welge, Chem. Phys. Letters, 33, 168 (1975).

21. R. Lesclaux, P. V. Khê, P. Dezauzier, and J. C. Soulignac, Chem. Phys. Letters, 35, 493 (1975).

22. S. Gordon, W. Mulac, and P. Nangia, J. Phys. Chem., 75, 2087 (1971).

23. K. Schofield, J. Chem. Phys. Ref. Data, 8, 723, (1979).

24. H. Kurasawa and R. Lesclaux, Chem. Phys. Letters, 66, 602 (1979).

25. C. W. Gear, Numerical Initial Value Problems in Ordinary Differential Equations, Prentice-Hall Inc., 1971.

26. M. R. Whitbeck, Private Communication.

27. H. Okabe, Photochemistry of Small Molecules, John Wiley and Sons, 1978.

28. R. F. Hampson, "Chemical Kinetic and Photochemical Data Sheets for Atmospheric Reactions," D.O.T. Report No. FAA-EE-80-17, 1980.

29. V. A. Lozovskii, V. A. Nadtochenko, O. M. Sarkisov, and S. G. Cheskis, Kinetica i. Kataliz., 20, 1118 (1979).

30. D. L. Bauch, R. A. Cox, P. J. Crutzen, R. F. Hampson, Jr., J. A. Kerr, J. Troe, and R. T. Watson, J. Phys. Chem. Ref. Data, 11, 393 (1982).

31. M. A. A. Clyne and P. M. Holt, J. Chem. Soc. Faraday Trans. II, 75, 569 (1979).

DISTRIBUTION LIST

Research Laboratories

W. G. Agnew	Executive Department
R. J. Blint	Physics Department
C. J. Dasch	Physics Department
R. E. Teets	Physics Department
R. C. Peterson	Engine Research
T. M. Sloane	Physical Chemistry
A. R. Sapre	Fuels and Lubricants Dept.
Technical Information Department (3)	

Patent Section

G. A. Grove